

Full Length Research Paper

Analysis of oil flow in fractured oil reservoir using carbondioxide (CO₂) foam injection

Minhee Choi, Junwoo Seo, Hyemin Park and Wonmo Sung*

Department of Natural Resources and Environmental Engineering, Hanyang University, 222 Wangsimni-ro, Seongdong-gu, Seoul 133-791, Korea.

Accepted 22 may, 2013

Most carbonate reservoirs are heterogeneous in terms of pore distribution and the matrix is extremely low permeable, hindering the flow of oil, while highly permeable fractures are the primary flow conduit. This study presents the hybrid discrete fracture network (DFN) approach to represent fracture network, more realistically, which is a continuum approach equipped with local grid refinement (LGR). The LGR is adapted at the cells that fractures are passing through, in order to describe the fracture width less than 0.1 ft. In this approach, control volume of the well lying on the fracture is extremely small and thus, in this study, four-leg horizontal well concept substitutes the vertical well with the use of equivalent well radius for overcoming the numerical convergence problem. The hybrid DFN approach was applied for CO₂-foam injection in fractured carbonate reservoirs to investigate the effect of conformance control. This foam injecting method yields more imbibition of CO₂-foam into low permeable matrix, which contains most of the oil. From the numerical results, it shows that the foam controls CO₂ velocity and this increases the contact time between CO₂ and the rock matrix since CO₂ mobility is controlled by foam, that decreases relative permeability of CO₂ and increases its viscosity.

Key words: Carbonate, fracture, local grid refinement, CO₂-foam, conformance control, discrete fracture network (DFN).

INTRODUCTION

Carbonate reservoirs account for over 40% of total worldwide oil reservoirs, and heavy oil contained in these is estimated to be 1.6 trillion bbl in place (Briggs, 1992; Das, 2007). Most carbonate reservoirs are heterogeneous, comprising fractures, vugs, and cavities. Also, the matrix has very low permeability, hindering the flow of heavy oil, while highly permeable fractures are the primary flow conduit. This renders the recovery process highly ineffective, and a large amount of oil is retained by the tight matrix after the application of primary and secondary recovery methods. Of current enhanced-oil-recovery (EOR) methods, CO₂ flooding has great

potential for recovering additional oil after water flooding. The advantage of CO₂ as an injection gas is its relatively low minimum miscibility pressure (MMP), making CO₂ applicable in a broad range of reservoirs (Stalkup, 1983). However, gravity override and viscous fingering caused by geological heterogeneity and unfavorable CO₂ mobility lead to poor macroscopic sweep efficiency and early CO₂ breakthrough.

The application of foam can reduce gas mobility, mitigate the effects of heterogeneity, and increase sweep efficiency (Liu et al., 2011). For the creation of foam, surfactant must be present. Foam can be injected into the

*Corresponding author. E-mail: wmsung@hanyang.ac.kr.

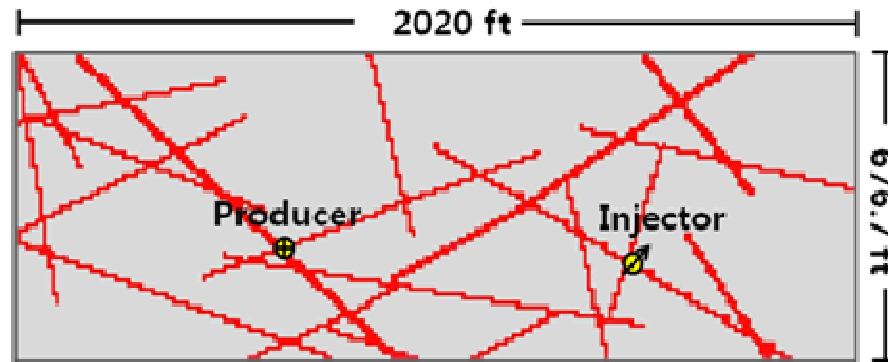


Figure 1. System description.

reservoir by co-injection of surfactant solution and gas, or by surfactant-alternating gas (SAG) injection. Foam moves through the porous media via the film network of bubbles, and gas moves through the system by breaking and by re-forming bubbles throughout the length of the flow path (Hirasaki, 1989). The stability of foam is a function of the surfactant type, surfactant concentration, foam quality, reservoir temperature, salinity, oil saturation, and other variables.

CO₂ foam reduces the mobility of CO₂ within the fracture network and decreases the velocity of CO₂ through the fractures, increasing the contact time between CO₂ and the carbonate rock matrix. This increases the imbibition of CO₂ into the low permeable matrix. Furthermore, with mobility control, foam diverts CO₂ and the surfactant solution to the tight matrix, where it can alter the wettability characteristics of the carbonate matrix from oil-wet to water-wet, causing more CO₂ foam to be imbibed into the matrix. Also, it reduces the interfacial tension (IFT) between the oil and water for release and mobilization of matrix oil, increasing the recovery factor.

Although several field studies and numerous laboratory tests with foam have shown some success (Heller et al., 1985; Hoefner et al., 1995; Holm et al., 1988), foams are a highly complex technology, both chemically and operationally, making them difficult to successfully apply in the oilfield (Sydansk and Romero-Zeron, 2011). Thus, prediction of CO₂ foam behavior in field-scale, especially for fractured carbonate reservoirs with a tight matrix still needs to be studied. In the present study, we conducted field-scale numerical simulations of CO₂ foam injection in fractured carbonate reservoirs with low permeable matrices containing heavy oil, using the hybrid discrete fracture network (DFN) approach. This approach represents fracture network more realistically, which is a continuum approach equipped with local grid refinement (LGR). The LGR is adapted at the cells that fractures are passing through, in order to describe the fracture width

less than 0.1 ft. Also, control volume of the well lying on the fracture is extremely small and thus, in this study, four-leg horizontal well concept substitutes the vertical well with the use of equivalent well radius for overcoming the numerical convergence problem. The hybrid DFN approach, which is free of the limitations of the dual porosity/dual permeability (DP/DK) model, allows the investigation of fluid transfer between a fracture and a matrix as well as fluid flow only through the fractures. The foam model in the simulator was used to apply the mobility reduction. In this study, we focused on determining the effect of several operational parameters on CO₂ foam behavior to control fast CO₂ flow through fractures and to improve oil flow in a rock matrix by considering the imbibition of CO₂ foam into the matrix.

SIMULATION SYSTEM

Simulation strategy and scenarios

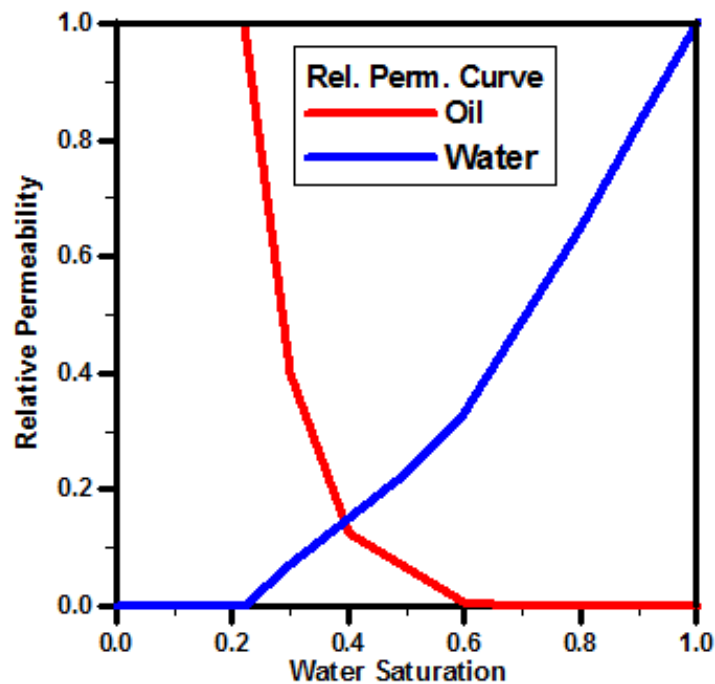
To analyze CO₂ foam behavior in a fractured carbonate reservoir, a two-dimensional model was constructed, as shown in Figure 1. Generally, a dual-porosity/dual-permeability (DP/DK) model is used to conduct the simulation in fractured reservoirs, including carbonates, but the directional property of each fracture cannot be described using this model (Muhammad, 2011). For this reason, we used the hybrid DFN approach in which it is possible to input permeability into each of the cells in the single-porosity (SP) model. Using this approach, we generated a fracture network, consisting of 19 fractures connected together, with matrix permeability of 1.0 md and fracture permeability of 2000 md.

CO₂ gas and surfactant solution were set up to co-inject and generate CO₂ foam under the reservoir condition. The wells were located on the connected fracture network, and the producer was specified by constant bottom-hole pressure while the injector was specified by constant rate to investigate the effect of injection rate. The total period of injection and production was 3 years, and the other input data in the model are listed in Table 1.

In fluid and rock properties, the oil-wet characteristic of carbonate rock is considered by the oil-water relative permeability curve (Figure 2). Also, because we assumed a dead-oil system without free gas and solution gas, the gas existing in the reservoir repre-

Table 1. Input data for the simulation study.

Parameter		Value
No. of Global Cell (X-Y)		13400 (200 × 67 × 1)
No. of LGR Cell (X-Y)		1569 (3 × 3 × 1)
Permeability [md]	Fracture	2000
	Matrix	1.0
Porosity		0.20
Initial Pressure [psia]		4000
Initial Oil Saturation		0.80
Initial Water Saturation		0.20
Depth [ft]		9000
Production Well BHP [psia]		3000
Injection Rate	Water (STBD)	40.0
	CO ₂ (MSCFD)	4.7754
Oil Density [lb/ft ³]		62.5
CO ₂ Density [lb/ft ³]		0.117
Surfactant Concentration [wt%]		0.001

**Figure 2.** The relative permeability curve for oil-wet carbonate reservoir.

sents only CO₂ gas, which has a surface density of CO₂. Once CO₂ gas is injected into the reservoir, CO₂ becomes miscible or immiscible with oil as it flows (Karaoguz et al., 1989; Shoab et al.,

2009). We assumed an immiscible process because oil has a high molecular weight in the case of heavy oil, making it difficult to develop miscibility with CO₂.

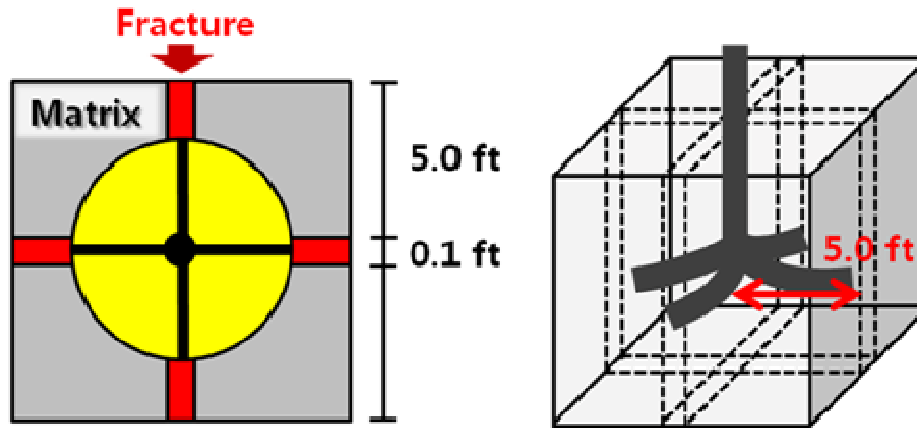


Figure 3. Multi-segment well in LGR fracture cell.

Hybrid discrete fracture network (DFN) approach

In the case of fractured system, local grid refinement (LGR) of the cells passing along the fractures was set up to describe a fracture aperture representing a realistic fracture size. From among the total 13,400 cells, which have dimensions of $200 \times 67 \times 1$, 1596 cells were used in LGR of 3×3 cells, and the fracture aperture was set to 0.1 ft (Figure 3). This resulted in increase of the grid cells number to be 26,168 cells, which is increasing by up to twice the original number of cells. Also, It is impossible to locate a vertical well on the fracture cell that can afford a practical flow rate because this cell has an extremely small size. Thus, as shown in Figure 3, a multi-segment well with four legs using the concept of equivalent well radius was adopted instead of vertical well to overcome the numerical convergence problem and to control the flow rate within the small cell volume.

Application of LGR technique is efficient for increasing the degree of accuracy with lower computational time and computer storage to obtain the solution. However, since the long and narrow cells lead to huge computing and numerical errors, extremely small size of time step, in which the initial time step size Δt_i is 0.00001 day (8 s), the maximum time step size Δt_{\max} is 0.1 day (2.4 h), and the minimum time step size Δt_{\min} is 0.01 day (14.4 min) was applied to control the convergence errors.

Foam model in simulator

In the foam module of the simulator, because flow of foam in a porous medium is highly complex, investigating and modeling the nature of foam generation and coalescence as well as its rheological and physical properties remains a challenge that requires further research. For this reason, the foam model used in this simulation study assumes a simple conservation equation (Eclipse® 100, 2012). Accordingly, the foam generation and breakage mechanism are not considered in detail, and the foam is modeled as a tracer that can be transported with the gas or the water phase, taking into account adsorption onto the rock surface (Emadi et al., 2011).

In this simplified simulation model, the effect of foam on gas mobility is modeled by reducing the gas relative permeability or

increasing the gas viscosity. A mobility reduction factor, M_{rf} , is applied to alter both end point of gas relative permeability and trapped gas saturation, and this factor is calculated as follows;

$$M_{rf} = \frac{1}{1 + (M_r \cdot F_1 \cdot F_2 \cdot F_3 \cdot F_4)} \quad (1)$$

where, F_1 accounts for various effects, such as F_1 for surfactant concentration, F_2 for water saturation, F_3 for oil saturation, and F_4 for gas velocity (Spirova et al., 2012). These dimensionless groups are suitably scaled by exponents e_s , e_o and e_c and weighting factor f_w under varying physical conditions. Each of F_i implies that

$$F_1 = \left(\frac{C_s}{C_s^r} \right)^{e_s}$$

$$F_2 = 0.5 + \frac{a \tan[f_w \cdot (S_w - S_w^l)]}{\pi}$$

$$F_3 = \left(\frac{S_o^m - S_o}{S_o^m} \right)^{e_o}$$

$$F_4 = \left(\frac{N_c^r}{N_c} \right)^{e_c}$$

In the above equations, C_s , S_w , S_o and N_c represent surfactant concentration, saturation of water, saturation of oil, and capillary number, respectively. Their corresponding critical values are denoted by C_s^r , S_w^l , S_o^m and N_c^r .

In addition, M_r is the reference mobility reduction factor obtained at maximum surfactant concentration and zero oil saturation. Usually, M_r has the range of 5 to 100. The gas relative permeability is then rescaled from k_{ro} to $(k_{ro} \cdot M_{rf})$ by the foam effect.

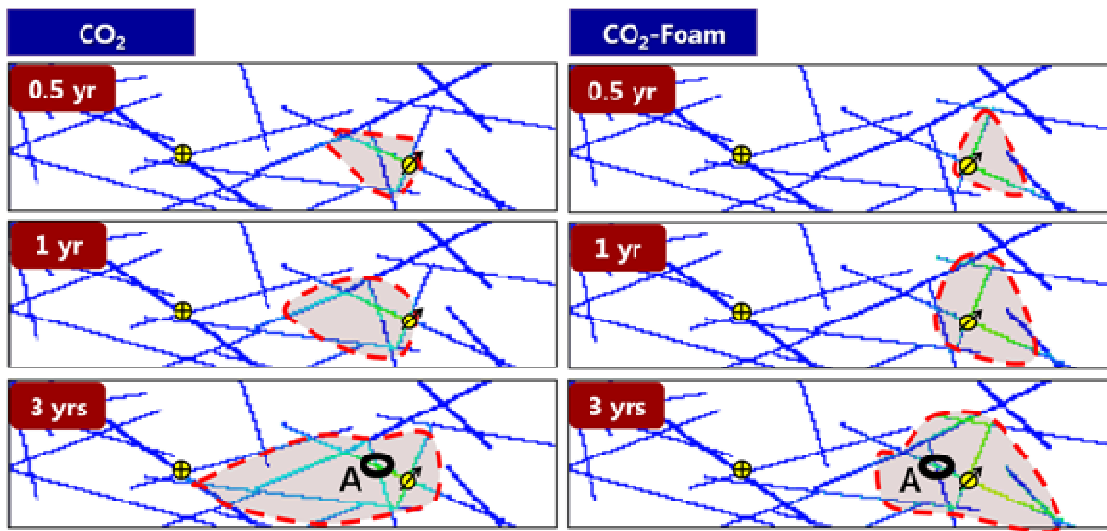


Figure 4. The CO₂ saturation distribution in fractured carbonate system.

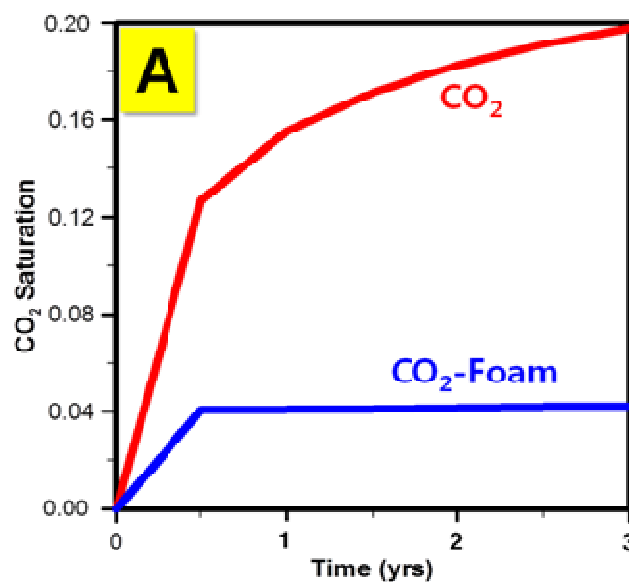


Figure 5. The CO₂ saturation change at location of "A".

RESULTS AND DISCUSSION

Oil flow in the matrix by CO₂ foam

To verify the effect of CO₂ foam injection with application of hybrid DFN approach using LGR on improving oil flow in the tight rock matrix, two simulation studies were conducted. First, we considered injection at 4.7754 MSCFD of CO₂ gas and 40 STBD of water with 0.001 wt% surfactant. A second process was used for

comparative analysis of CO₂ flow velocity, which considered continuous injection of only CO₂ gas at 5 MSCFD (Figure 4). Figure 4 shows the CO₂ saturation distribution over 3 years; CO₂ quickly flows through the fractures toward the production well for continuous CO₂ injection compared with the case of CO₂ foam injection. We set point "A" between the two wells to examine the foam effect on flow control by observing the CO₂ saturation change. As shown in Figure 5, CO₂ saturation hardly increases after 0.5 year of CO₂ foam injection,

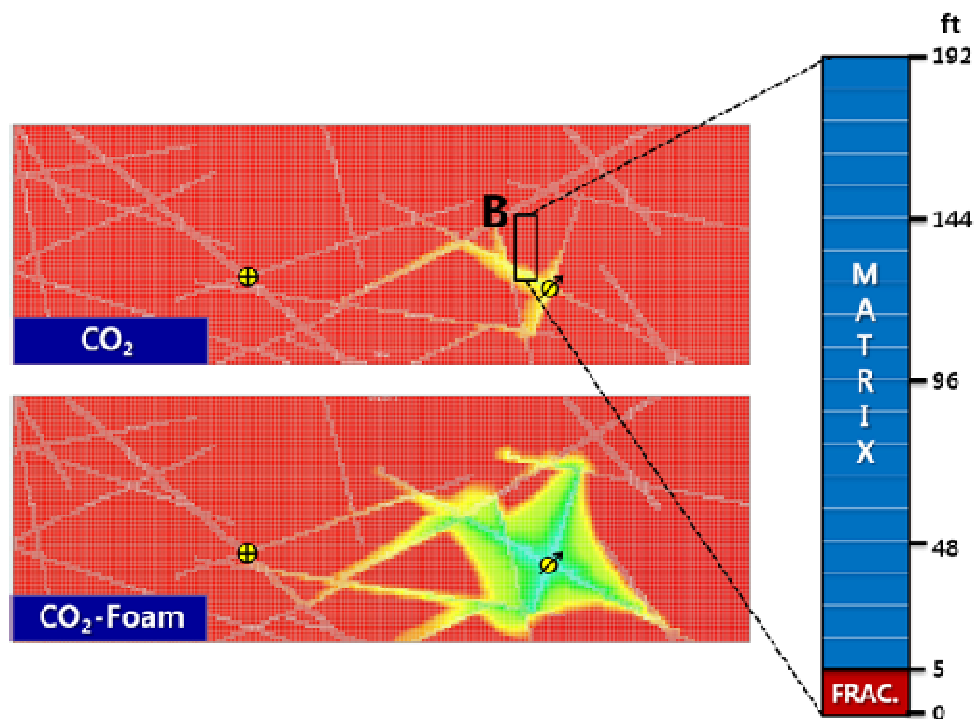


Figure 6. The oil saturation distribution at 1 year of production.

while CO_2 saturation consistently increases for the case of continuous CO_2 injection. This is because the mobility of gas-phase CO_2 is higher than that of liquid-phase foam, producing a greater flow velocity. It was shown that injection pressure for CO_2 foam injection with lower mobility has more than doubled compared to gas-phase CO_2 injection with higher mobility. This trend was also observed in the oil saturation distribution shown in Figure 6. For CO_2 foam injection, the sweep efficiency with oil improved because the liquid-phase foam enables capillary imbibition into the matrix as well as velocity control of fracture flow; for CO_2 injection, CO_2 gas preferentially moves through the fractures. With mobility control, foam diverts CO_2 and the surfactant solution to the tight matrix, where it can alter the wettability characteristics of the carbonate matrix from oil-wet to water-wet, causing more CO_2 foam to be imbibed into the matrix. Also, it reduces the interfacial tension (IFT) between the oil and water for release and mobilization of matrix oil, increasing the recovery factor (Fjelde et al., 2008; Shramm, 1994).

To analyze fluid imbibition into the rock matrix and improvement in oil flow in detail, the saturation change was measured at an arbitrary point “B”. Figure 6 shows that section “B” consists of 5 ft of fracture and the remaining matrix, totaling 192 ft long. As indicated in

Figure 7, when only CO_2 was injected, oil and CO_2 saturation in the rock matrix started to change at 6 months, and, moreover, the changes reached just 20% of the total distance after 3 years. On the other hand, when CO_2 foam was injected (Figure 8), the change started at 1 month with a rapid increase in foam concentration and, accordingly, a decrease in oil saturation. Because the contact time and area between the injected CO_2 foam and the rock matrix increased, the oil in the rock matrix with a large area was displaced. Thus, the oil saturation change reached the total distance of 192 ft between 12 months and 18 months.

As a consequence of the above results, the curves in Figure 9 for average matrix oil saturation (except for fractures), indicate that both primary oil recovery by natural production and the case of simple CO_2 injection changed slightly, whereas CO_2 foam injection changed 10% from 0.8 to 0.72, confirming that CO_2 foam injection greatly improves oil flow in rock matrix.

Conclusively, as shown in production data at the well (Figure 10), the oil production rate for CO_2 foam injection is enhanced about five times compared to only CO_2 injection. Also, when CO_2 was injected, the CO_2 breakthrough time (BT) was 300 days. However, when CO_2 foam injection was applied, CO_2 breakthrough did not occur during the total production years, indicating that

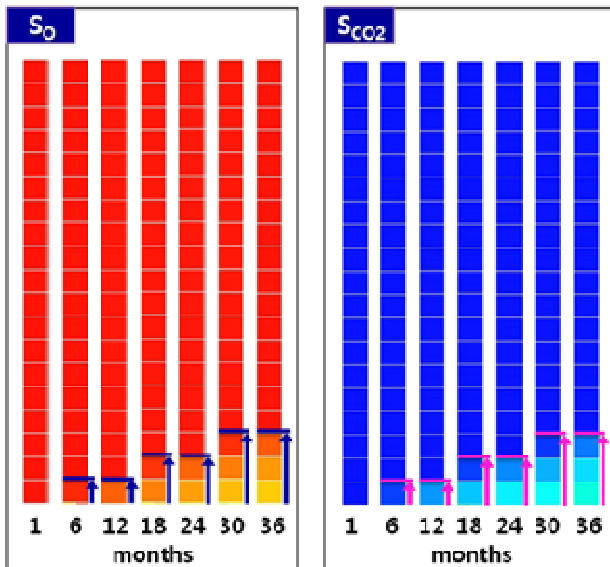


Figure 7. The changes of oil and CO₂ saturations at location of "B" in the case of CO₂ injection.

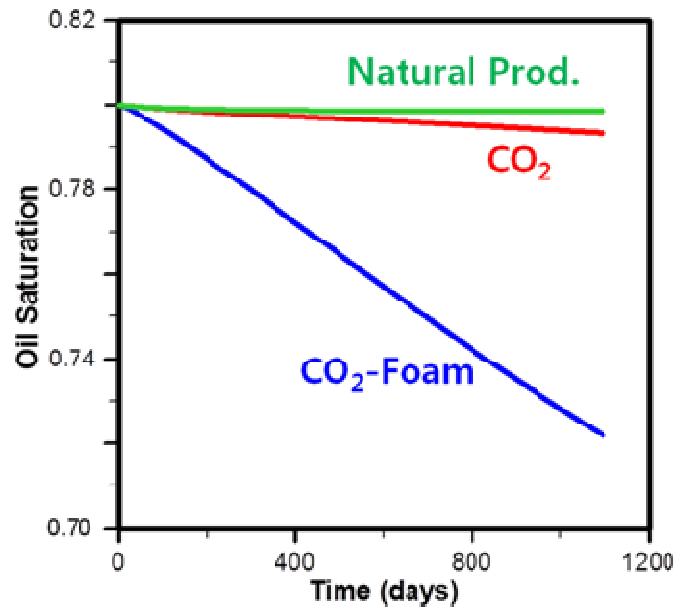


Figure 9. The average matrix oil saturation.

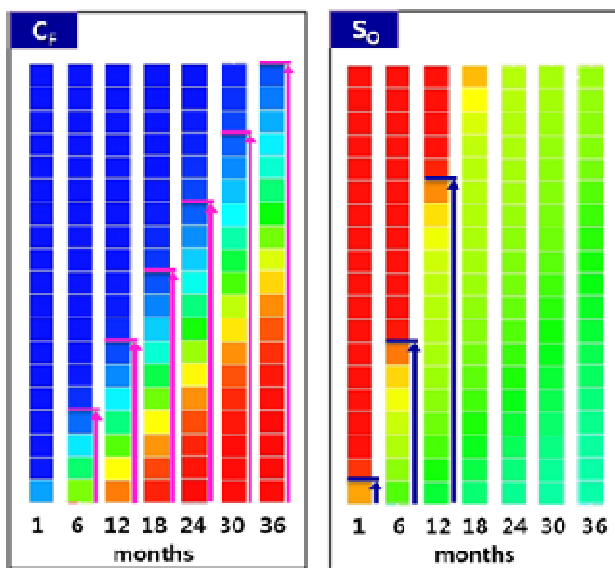


Figure 8. The changes of foam concentration and oil saturation at location of "B" in the case of CO₂ foam injection.

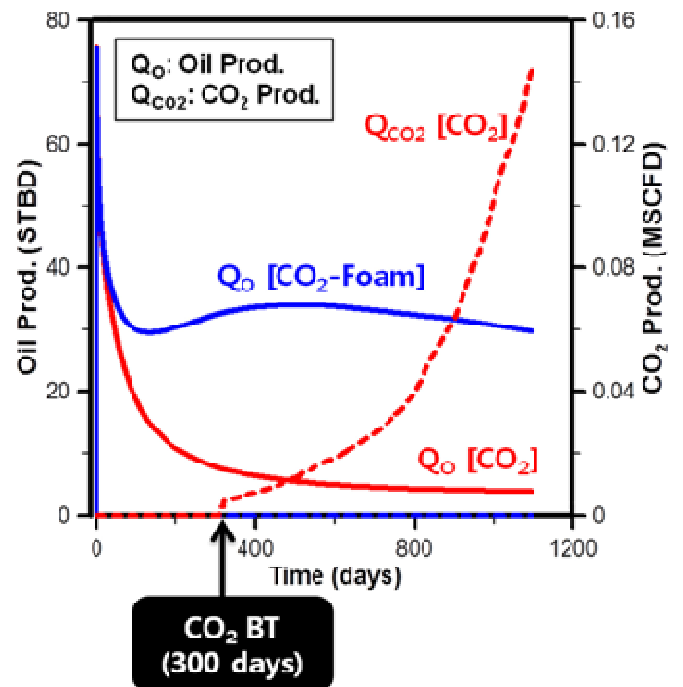


Figure 10. The oil production rate and CO₂ BT for the cases of CO₂ and CO₂ foam injection.

fracture flow was well-controlled by CO₂ foam injection, preventing early BT of CO₂.

Effect of injection fluid

It is important to determine which fluid plays a dominant

role in promoting the foam effect when water, including surfactant, and CO₂ gas are co-injected to generate

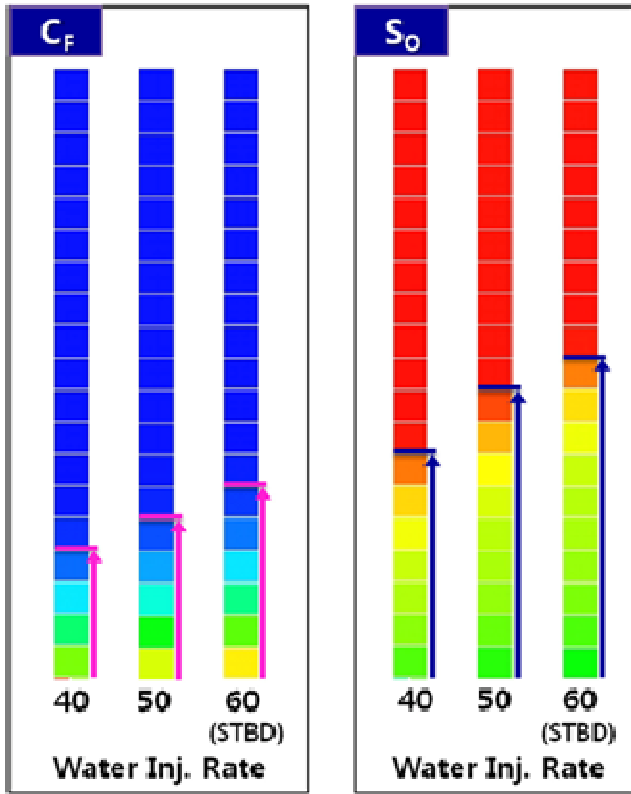


Figure 11. The changes of foam concentration and oil saturation at location of “B” for various cases of water injection rate at 6 months of production.

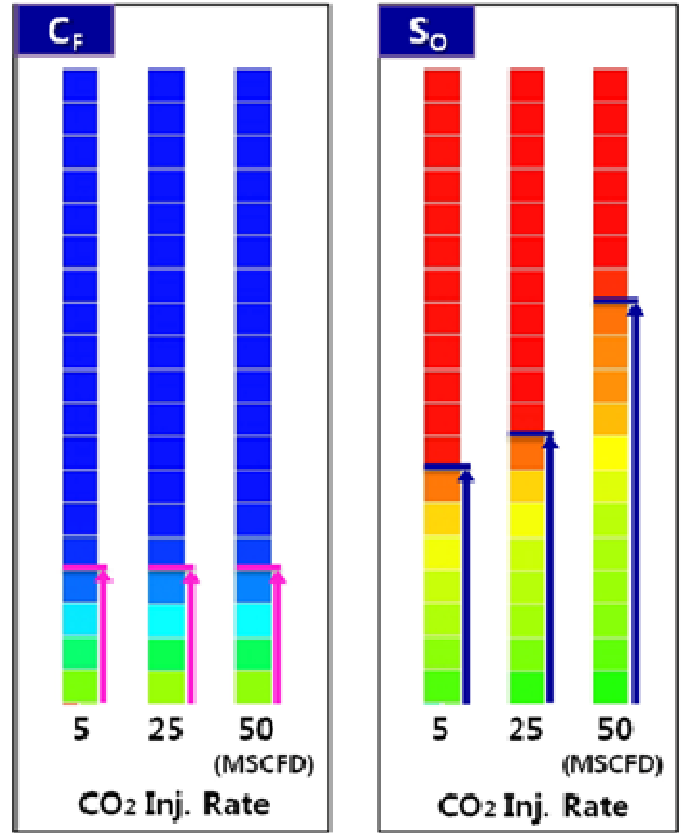


Figure 13. The changes of foam concentration and oil saturation at location of “B” for various cases of CO₂ injection rate at 6 months of production.

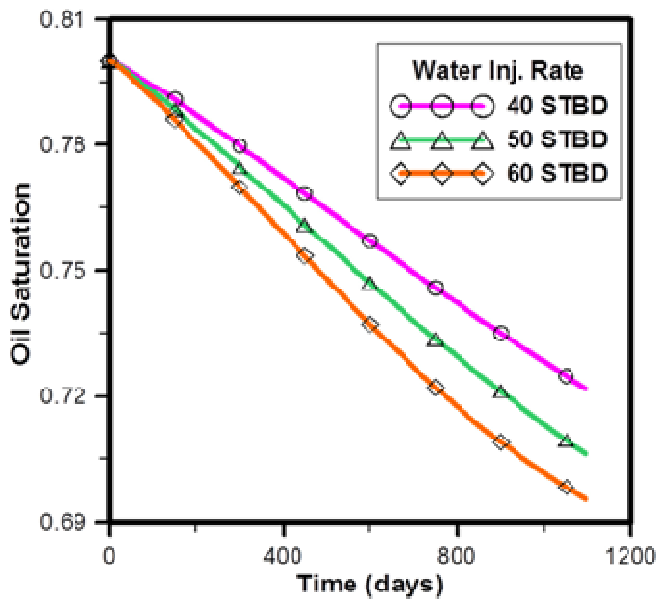


Figure 12. The average matrix oil saturations for various cases of water injection rate.

CO₂ foam under the reservoir condition.

For this determination, three simulation runs were performed with water rates ranging from 40 to 50 and to 60 STBD with 0.001 wt% surfactant, while the co-injected CO₂ rate was fixed at 5 MSCFD. Figure 11 shows that higher water injection rates led to higher foam concentrations, decreasing the oil saturation deep in the rock matrix after 6 months. This means that, as the water (including surfactant) injection rate increases, more CO₂ foam is imbibed into the rock matrix, and rapid flow into fractures is controlled, displacing a large portion of oil remaining in the matrix. As a result, the average matrix oil saturation (Figure 12) further decreased when the water injection rate was high.

In sequence, three different CO₂ injection rates were considered: 5, 25, and 50 MSCFD with the same bottom-hole pressure at the injection well for the three simulations above according to water rate. The water injection rate was maintained at 40 STBD with 0.001 wt% surfactant. Figure 13 shows that greater CO₂ injection rates resulted in less oil saturation deep in the rock matrix

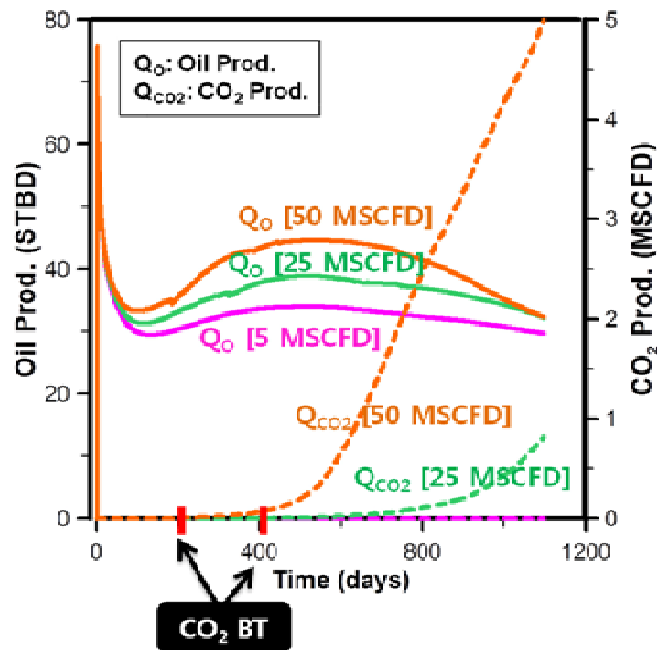


Figure 14. The oil production rate and CO₂ BT for various cases of CO₂ injection rate.

after 6 months, while the foam concentration did not change. Also, the CO₂ BT at the production well occurred early when the CO₂ rate was high (Figure 14). This indicates that an increase in amount of injected CO₂ did not affect fracture flow control via CO₂ foam; the result shown in Figure 13, in which matrix oil saturation was reduced, was likely due to the effect of increased total injection rate. That is, as the CO₂ injection rate increases, the amount of CO₂ imbibed into the rock matrix increases and displaces more oil from the matrix. However, it hardly influences foam flow and thus does not control rapid flow through the fractures on the contrary to the case of increasing water rates.

Effect of surfactant concentration

Since the surfactant is essential for generating foam, it is important to determine the proper surfactant concentration (Zuta et al., 2011). To investigate the effect of surfactant concentration with application of hybrid DFN approach using LGR, two comparative simulation runs were performed with a fixed CO₂ rate of 5 MSCFD and a water rate of 40 STBD with 0.01 and 1.0 wt% surfactant for 6 years.

Figure 15 shows the CO₂ saturation distribution in fractures, showing the effect on fracture flow control. In the case of high surfactant concentration of 1.0 wt%, CO₂ saturation was distributed densely within a narrow radius

range compared to the case of low concentration of 0.01 wt%. Thus, CO₂ flow velocity in fractures is effectively slowed by high surfactant concentration, increasing the contact time between CO₂ and the rock matrix. In addition, Figure 16 shows that the CO₂ gas viscosity was held at a higher value for the case of higher surfactant concentration because this facilitated CO₂ foam formation. The viscosity change over time is caused with increases or decreases in pressure and temperature of the reservoir (Hirasaki et al., 1985). Consequently, Figure 17 shows that the CO₂ BT occurred at 1250 days with 11.2 pore volume of injection and 1600 days with 14 pore volume of injection for each case, indicating that BT was delayed with the high surfactant concentration.

Conclusion

A simulation for CO₂ foam injection in fractured carbonate reservoirs was performed to investigate the effect of foam on both rapid flow control in fractures and improved oil flow in a rock matrix. For the simulations, the fracture system was described using LGR and the hybrid DFN approach in which the fracture aperture is represented more realistically in comparison with existing works. The main results and conclusions are as follows:

1. Foam controls the CO₂ flow velocity and increases the contact time between CO₂ and the rock matrix. Hence,

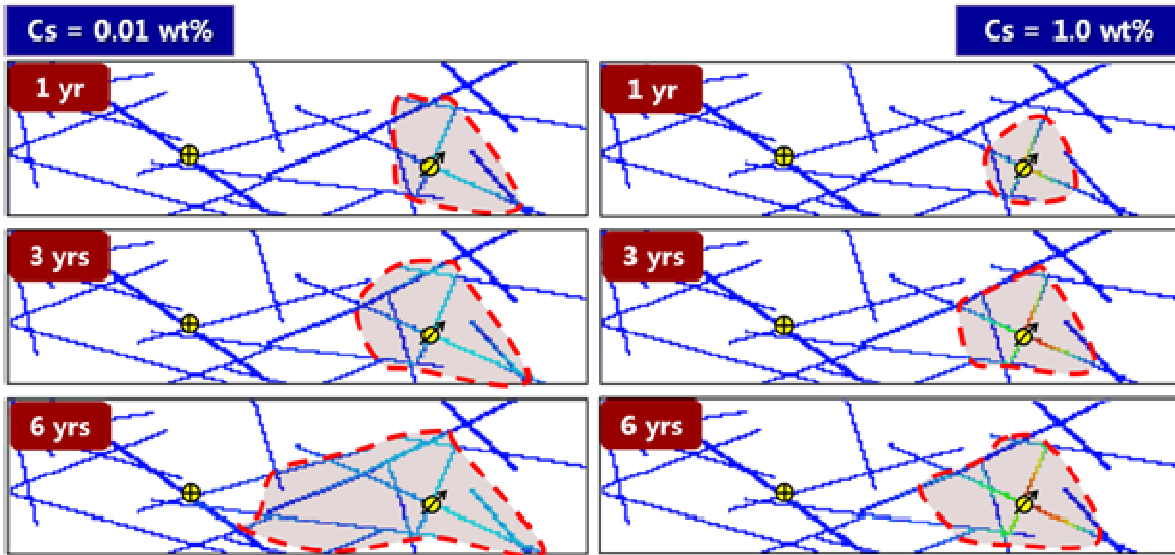


Figure 15. The CO₂ saturation distributions with surfactant concentrations.

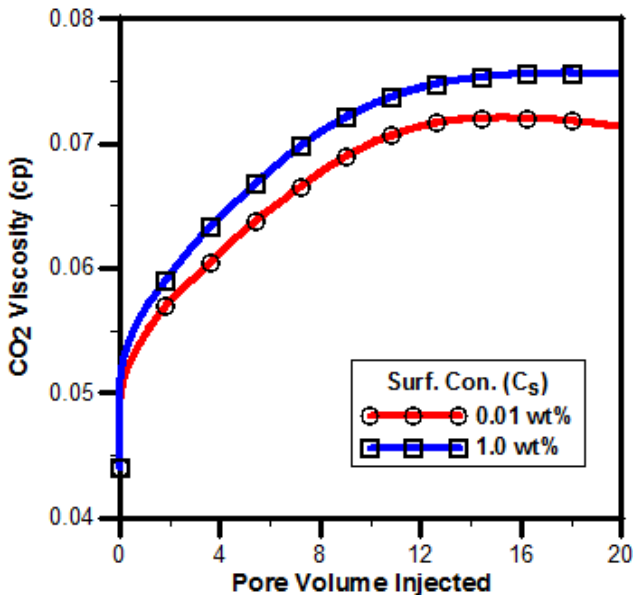


Figure 16. The CO₂ viscosity changes with surfactant concentrations.

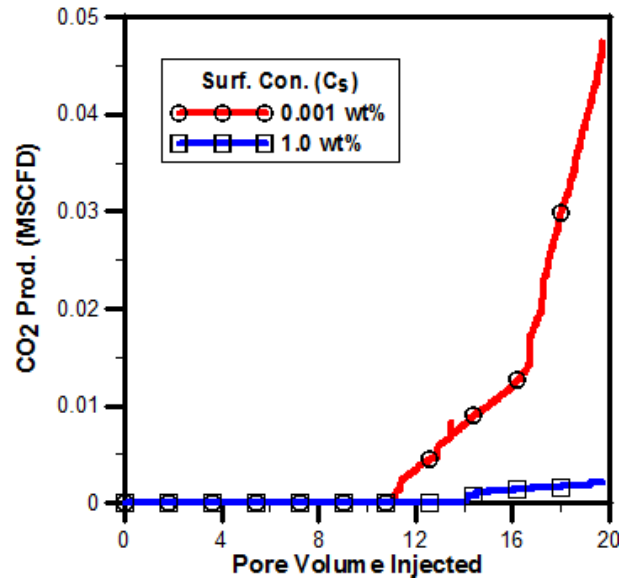


Figure 17. The CO₂ BT with surfactant concentrations.

injected CO₂ foam can be adsorbed and imbibed into the matrix, improving oil flow from the matrix. This is because CO₂ mobility is controlled by foam, which decreases CO₂ relative permeability and increases its viscosity.

2. During 3 years of production, the BT of the injected CO₂ was occurred at 300 days in the case of only CO₂ injection, meanwhile CO₂ breakthrough was not observed at producer when CO₂ foam was applied, indicating that

foam prevents early CO₂ breakthrough.

3. The trend of decreasing oil saturation indicated that CO₂ foam injection is more effective for improving oil flow in the matrix; the decrease in oil saturation reached 16% of the total distance after 3 years for CO₂ injection, but it reached the total distance at 1.5 years for CO₂ foam injection.

4. In both cases of increasing water injection rate (with

the same surfactant concentration) and increasing CO₂ injection rate, the oil flow in the rock matrix was enhanced. However, CO₂ BT was occurred earlier, and oil production was lowered with increasing CO₂ injection rate. Therefore, the optimal design for injection rate is essential by considering injecting fluid in advance.

5. Higher surfactant concentration for CO₂ foam resulted in greater CO₂ viscosity. Thus, CO₂ flow velocity can be controlled effectively, resulting in increased oil production and retardation of CO₂ BT. Thus, formulation-related research should be continuously carried out in order to design cost-effective surfactant based EOR which requires an economic viability.

ACKNOWLEDGMENTS

This work was supported by a grand from the Energy Efficiency & Resources of Korea Institute of Energy Technology Evaluation and Planning (KETEP), funded by the Korean Ministry of Knowledge Economy (No.2010201010092A).

REFERENCES

- Briggs PG, Beck DI, Black CJJ, Bissel R (1992). Heavy Oil from Fractured Carbonate Reservoirs. *SPE*. 7(2): 173-179.
- Das S (2007). Application of Thermal Recovery Processes in Heavy Oil Carbonate Reservoirs. Paper SPE 105392 presented at the 15th SPE Middle East Oil and Gas Show and Conference, Bahrain International Exhibition Centre, Kingdom of Bahrain, 11-14 March.
- Eclipse® 100 (2012). Technical Description. Schlumberger.
- Emadi A, Sohrabi M, Jamiolahmady M, Ireland S, Rørvik G (2011). Mechanistic Study of Improved Heavy Oil Recovery by CO₂-Foam Injection. Paper SPE 143013 presented at the SPE Enhanced Oil Recovery Conference, Kuala Lumpur, Malaysia, 19-21 July.
- Fjelde I, Zuta J, Olawale VD (2008). Oil Recovery from Matrix during CO₂-Foam Flooding of Fractured Carbonate Oil Reservoirs. Paper SPE 113880 presented at the 2008 SPE Europec/EAGE Annual Conference and Exhibition, Rome, Italy, 9-12 June.
- Heller JP, Boone DA (1985). Field Test of CO₂ Mobility Control at Rock Creek. Paper SPE 14395 presented at the 60th SPE Annual Technical Conference and Exhibition, Las Vegas, USA, 22-25 September.
- Hirasaki GJ (1989). Supplement to SPE 19505, The Steam-Foam Process-Review of Steam-Foam Process Mechanisms. Paper SPE 19518, 19 April.
- Hirasaki GJ, Lawson JB (1985). Mechanisms of Foam Flow in Porous Media: Apparent Viscosity in Smooth Capillaries. Paper SPE 12129 presented at the 1983 SPE Annual Technical Conference and Exhibition, San Francisco, USA, 5-8 October.
- Hoefner ML, Evans EM (1995). CO₂ Foam: Results From Four Developmental Field Trials. Paper SPE 22787 presented at the 1994 SPE/DOE Symposium on Improved Oil Recovery, Tulsa, Oklahoma, USA, 17-20 April.
- Holm LW, Garrison WH (1988). CO₂ Diversion With Foam in an Immiscible CO₂ Field Project. *SPE* 3(1):112-118.
- Karaoguz D, Issever K, Pamir N, Tirek A (1989). Performance of a Heavy-Oil Recovery Process by an Immiscible CO₂ Application, Bati Raman Field. Paper SPE 18002 presented at the SPE Middle East Oil Technical Conference and Exhibition, Manama, Bahrain, 11-14 March.
- Liu MK, Rossen WR (2011). Sweep Efficiency in CO₂ Foam Simulations With Oil. Paper SPE 142999 presented at the SPE Europec/EAGE Annual Conference and Exhibition, Vienna, Austria, 23-26 May.
- Muhammad S (2011). Flow and Transport in Porous Media and Fractured Rock, 2nd Ed. WILEY-VCH, Weinheim.
- Shoab S, Hoffman BT (2009). CO₂ Flooding the Elm Coulee Field. Paper SPE 123176 presented at the 2009 SPE Rocky Mountain Petroleum Technology Conference, Denver, Colorado, USA, 14-16 April.
- Shramm LL (1994). Foams: Fundamentals and Applications in the Petroleum Industry. American Chemical Society, Washington DC.
- Spirov P, Rudyk SN, Khan AA (2012). Foam Assisted WAG, Snorre Revist with Foam Screening Model. Paper SPE 150829 presented at the SPE North Africa Technical Conference and Exhibition, Cairo, Egypt, 20-22 February.
- Stalkup FI (1983). Miscible Displacement. *SPE Monogr. Ser.* 8(4):815-826.
- Sydansk RD, Romero-Zeron L (2011). Reservoir Conformance Improvement. Society of Petroleum Engineers, USA
- Zuta J, Fjelde I (2011). Mechanistic Modeling of CO₂-Foam Processes in Fractured Chalk Rock: Effect of Foam Strength and Gravity Forces on Oil Recovery. Paper SPE 144807 presented at the SPE Enhanced Oil Recovery Conference, Kuala Lumpur, Malaysia, 19-21 July.